



**HAL**  
open science

## Understanding ageing mechanisms of porous carbons in non-aqueous electrolytes for supercapacitors applications

Yinghui Liu, Bénédicte Réty, Camelia Ghimbeu, Benoît Soucaze-Guillous,  
Pierre-Louis Taberna, Patrice Simon

### ► To cite this version:

Yinghui Liu, Bénédicte Réty, Camelia Ghimbeu, Benoît Soucaze-Guillous, Pierre-Louis Taberna, et al.. Understanding ageing mechanisms of porous carbons in non-aqueous electrolytes for supercapacitors applications. *Journal of Power Sources*, 2019, 434, pp.226734. 10.1016/j.jpowsour.2019.226734 . hal-02383704

**HAL Id: hal-02383704**

**<https://hal.science/hal-02383704>**

Submitted on 27 Mar 2020

**HAL** is a multi-disciplinary open access archive for the deposit and dissemination of scientific research documents, whether they are published or not. The documents may come from teaching and research institutions in France or abroad, or from public or private research centers.

L'archive ouverte pluridisciplinaire **HAL**, est destinée au dépôt et à la diffusion de documents scientifiques de niveau recherche, publiés ou non, émanant des établissements d'enseignement et de recherche français ou étrangers, des laboratoires publics ou privés.



## Open Archive Toulouse Archive Ouverte (OATAO)

OATAO is an open access repository that collects the work of Toulouse researchers and makes it freely available over the web where possible

This is an author's version published in: <http://oatao.univ-toulouse.fr/25595>

**Official URL:** <https://doi.org/10.1016/j.jpowsour.2019.226734>

**To cite this version:**

Liu, Yinghui  and Réty, Bénédicte and Matei Ghimbeu, Camélia and Soucaze-Guillous, Benoît and Taberna, Pierre-Louis  and Simon, Patrice   
*Understanding ageing mechanisms of porous carbons in non-aqueous electrolytes for supercapacitors applications.* (2019) Journal of Power Sources, 434. 226734. ISSN 0378-7753

Any correspondence concerning this service should be sent to the repository administrator: [tech-oatao@listes-diff.inp-toulouse.fr](mailto:tech-oatao@listes-diff.inp-toulouse.fr)

# Understanding ageing mechanisms of porous carbons in non-aqueous electrolytes for supercapacitors applications

Yinghui Liu<sup>a,b</sup>, Bénédicte Réty<sup>b,c,d</sup>, Camélia Matei Ghimbeu<sup>b,c,d</sup>, Benoît Soucaze-Guillous<sup>f</sup>, Pierre-Louis Taberna<sup>a,b</sup>, Patrice Simon<sup>a,b,e,\*</sup>

<sup>a</sup> CIRIMAT, Université de Toulouse, CNRS, INPT, UPS, 118 route de Narbonne, 31062, Toulouse, France

<sup>b</sup> Réseau sur le Stockage Electrochimique de l'Energie (RS2E), FR CNRS 3459, 80039, Amiens, France

<sup>c</sup> Université de Haute-Alsace, Institut de Science des Matériaux de Mulhouse (IS2M) CNRS UMR 7361, F-68100, Mulhouse, France

<sup>d</sup> Université de Strasbourg, F-67081, Strasbourg, France

<sup>e</sup> Institut Universitaire de France, 1 rue des Ecoles, Paris, 75003, France

<sup>f</sup> Technocentre Renault, 1 avenue du Golf, API: TCR RUC 1 82, F-78084, Guyancourt, France

## HIGHLIGHTS

- Presence of water in the electrolyte catalyzes the ageing of supercapacitor.
- Electrochemical ageing causes carbon oxidation and forms surface functional groups.
- By-products of BF<sub>4</sub> hydrolysis react with acetonitrile to form soluble oligomers.
- Carbon surface functional groups plays an important role in the ageing mechanism.

## ARTICLE INFO

### Keywords:

Supercapacitor ageing  
Temperature-programmed desorption coupled with mass spectrometry technique  
Surface oxygen functional group  
Activated carbon oxidation  
Oligomer

## ABSTRACT

Two activated porous carbon powders with different surface functional groups content have been electrochemically polarized in tetraethylammonium tetrafluoroborate (Et<sub>4</sub>NBF<sub>4</sub>) in acetonitrile electrolyte to study their ageing mechanism as supercapacitor electrodes. Temperature-programmed desorption coupled with mass spectrometry technique (TPD-MS) is used to track the change of carbon surface chemistry – surface functional groups and/or adsorption of degradation products occurring upon polarizations. A potentiostatic study of the carbons in a two-compartment cell unveil the catalytic role of water in the ageing mechanism. Combining these results with our previous work, we propose different scenarios to depict the ageing mechanisms of the two carbons. For carbon A, hydrolysis of BF<sub>4</sub> at the positive electrode leads to carbon oxidation together with soluble poly-acetonitrile oligomer occurred from reaction between BF<sub>4</sub><sup>\*</sup> radicals and acetonitrile. Ageing mechanism is also assumed to set off with the hydrolysis of BF<sub>4</sub> for carbon B; but, in here the formed oligomers react with acid functional groups present at the carbon surface to form a protective, passive-like layer at both positive and negative electrodes which hampers a further electrode ageing.

## 1. Introduction

Electrochemical Capacitors (ECs), also known as Supercapacitors, were firstly introduced in 1957 by H. Becker [1] as energy storage devices. ECs can store high energy density compared to conventional dielectric capacitors and can harvest/deliver high power for tens of seconds which make them useful in applications ranging from power electronics to transportation (stop/start function in automobiles, braking energy recovery in trams and buses, etc. And power grids

[2–4]). Porous carbon-based ECs are the most advanced and competitive candidates to date for industrial applications. So far, only small attention has been paid to the study of ageing mechanisms of supercapacitor electrodes during long term cycling [5–7]. However, understanding the ageing mechanism of carbon-based supercapacitors is of high importance for safety and security reasons as well as for further optimization of EC performance particularly for long term utilization [8].

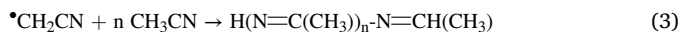
Among the few papers dealing with supercapacitor's ageing mechanisms, Azaïs et al. [5] studied the ageing of porous carbons in 1.5 M

\* Corresponding author. CIRIMAT, Université de Toulouse, CNRS, INPT, UPS, 118 route de Narbonne, 31062, Toulouse, France.

E-mail address: [simon@chimie.ups-tlse.fr](mailto:simon@chimie.ups-tlse.fr) (P. Simon).

tetraethylammonium tetrafluoroborate (Et<sub>4</sub>NBF<sub>4</sub>) in acetonitrile (ACN) electrolyte during constant potential polarizations using NMR and XPS spectroscopies. They proposed that the ageing of carbon-based supercapacitor electrode operating in non-aqueous electrolyte is related to the decomposition of the electrolyte onto the surface of active carbon sites (surface defects). Two types of carbons, Maxsorb and OPTI, were analyzed. OPTI carbon is a synthetic carbon made from the carbonization of a phenolic resin and then activated by water steam. Maxsorb carbon is prepared from KOH activation at 850 °C of petroleum pitch. X-ray photoelectron spectroscopy (XPS) and NMR spectroscopy analysis showed that the presence of acid functional groups on the carbon surface degrades the performance of the supercapacitors, especially in terms of ageing. Also, they suggested that the presence of water is one of the causes of supercapacitor ageing [5]. Based on the work of Azais et al., using the same electrolyte, by Raman spectroscopy, Zhu et al. [6] have shown that an amorphization of coconut shell-based carbons occurred as a result of electrochemical ageing which consisted in a constant potential polarization at 2.9 V for 45 days. XPS spectroscopy measurements evidenced the presence of nitrogen, fluorine and oxygen on the surface of aged carbons which was further assigned, by infrared spectroscopy analysis, to the presence of traces of pyridine (C=N), amines (C-NH<sub>2</sub>), polyacetonitrile  $[-N=C(CH_3)]_n^-$  and amides. These molecules were assumed to result from the polymerization of acetonitrile present both at the anode and at the cathode [6]. Such ageing is also favored by the formation of BF<sub>3</sub> and HF from the hydrolysis of (Et<sub>4</sub>NBF<sub>4</sub>) salt of the electrolyte in presence of water trace, which can further oxidize the carbon surface [9]. These results obtained in laboratory supercapacitor cell were later confirmed by Bittner et al. [7] who carried out similar analyzes using commercial supercapacitor cells. In particular, they evidenced by XPS analysis the presence of covalent nitrogen at the surface of the carbon, probably due to the existence of polyacetonitrile  $[-N=C(CH_3)]_n^-$ .

Later, Bittner et al. [7] et Tourillon et al. [10] proposed the formation of oligomers from the interaction between BF<sub>4</sub><sup>•</sup> radicals and acetonitrile according to following equations where BF<sub>4</sub><sup>•</sup> radicals are generated at high voltage, which set off the formation of polyacetonitrile through reaction (2) and (3) [10]:



Recently, we reported about the understanding of the ageing mechanisms of supercapacitor electrodes assembled with two different carbons A and B [8]. From electrochemical characterizations, we identified two different ageing mechanisms upon cycling: while a commercial activated carbon (carbon A) presented a continuous ageing with a constant decrease of the capacitance and an increase of the series resistance, carbon B (porous carbon used for water purification) ageing was identified by a constant capacitance associated with an increase of the series resistance after several weeks of cycling. The analysis of the ionic diffusion coefficient change during cycling confirmed the difference in ageing mechanisms, while Thermogravimetry – Infrared Spectroscopy (TG-IR) Coupled Analysis and Raman spectroscopies revealed the creation of defects in carbon A structure. Furthermore, in both carbons (A and B), structural modifications were found to be more significant at the positive electrode. However, these results fell short to picture out clearly ageing mechanisms.

In this study, focused on the same carbon A and B, as mentioned in our previous work, we used Temperature-Programmed Desorption coupled with Mass Spectrometry (TPD-MS) technique to get a better view of the porous carbon surface chemistry change upon ageing. Together with our previous results [8], this study brings out new evidences allowing to get a better understanding of the ageing mechanisms of these two different carbons during cycling.

## 2. Experimental

### 2.1. Electrochemical characterizations

#### 2.1.1. Swagelok supercapacitor's ageing study

Experimental details of cell assembly and electrochemical ageing have been detailed elsewhere [8]. Two activated carbons, A and B, were tested in this study [8]. Carbon A is the YP-50F commercial microporous carbon (Kuraray company) used for supercapacitor applications. Carbon B is a porous carbon used for water purification applications. Gas sorption analysis has been carried out using Ar gas at 77 K. Density functional theory (DFT) kernels have been used, which are the most up-to-date software analysis to extract porosity data from gas sorption isotherms for meso- and microporous carbons and effectively avoid the fundamental limitations of the BET theory. Table 1 below summarizes the characteristics of the two porous carbons [11].

As observed in Table 1, carbon A is mainly microporous (92 %vol. of micropores), within 49 %vol. are ultra-micropores (pore size smaller than 1 nm); on the other hand, Carbon B exhibit a broader pore size distribution since has a microporous porous volume of 66 %vol., including 32 %vol. of ultra-microporosity (pore size smaller than 1 nm).

Carbon electrodes were prepared by mixing activated carbon powder with PTFE binder [8]. Porous carbon films of 15 mg cm<sup>-2</sup> were prepared. 2-electrode Swagelok<sup>®</sup> cells were assembled in glove box by using 2 porous carbons disks as the electrodes, platinum disks for current collectors and a cellulose membrane as the separator. Electrolyte used for both cells was 1.5 M Et<sub>4</sub>NBF<sub>4</sub> (99%, ACROS Organics<SUP>TM</SUP>) dissolved in acetonitrile (HPLC Gradient, ACROS Organics<SUP>TM</SUP>). Supercapacitors cells using carbon A and B will be respectively referred as supercapacitor A (SC A) and supercapacitor B (SC B).

The supercapacitor cells (SCs) were tested under an accelerated electrochemical ageing process. In this process, one ageing cycle consisted of 12 h of a potentiostatic hold, called “floating”, followed by 6 galvanostatic cycles, called “check-up”. The capacitance and the series resistance were measured during the discharge portion at the 6th galvanostatic cycles of each “check-up”. End-of-life criteria was set as follows: an increase of 500% of the resistance or a capacitance loss of 50%.

As soon as the end-of-life criteria was reached, supercapacitor cells were disassembled, aged carbon electrode films were washed in 20 mL of acetonitrile (99.9%, Extra Dry, AcroSeal™, ACROS Organics™) then put in a Nalgene Centrifuge Tube for centrifugation. Carbons were washed by centrifugation at 3000 rpm for 1 h (SIGMA Type Model 3-18 equipment); procedure was repeated 3 times by renewing acetonitrile each time. Then, aged electrodes were dried for 1 h at 120 °C under vacuum before being analyzed by following methods.

#### 2.1.2. Ageing study of a cell with two separate compartments

Following original work from Ishimoto et al. [12], we used a two-compartment electrolyte cell, separated by a fritted glass with a porosity of 5 μm diameter, in order to isolate the negative (catholyte) and positive (anolyte) compartments during ageing to state about the difference of ageing between the two polarities. Water content was

**Table 1**  
DFT surface area of two porous carbons and their porous volumes according to pore size.

Carbon	DFT Surface Area (m <sup>2</sup> .g <sup>-1</sup> )	Total pore volume (cm <sup>3</sup> .g <sup>-1</sup> )	Pore volume > (2 nm) (cm <sup>3</sup> .g <sup>-1</sup> )	Pore volume (1 nm - 2 nm) (cm <sup>3</sup> .g <sup>-1</sup> )	Pore volume (<1 nm) (cm <sup>3</sup> .g <sup>-1</sup> )
A	1750	0.79	0.07	0.33	0.39
B	1297	0.76	0.26	0.26	0.24

measured using a Karl Fisher (KF 899 Coulometer, Metrohm). Glass beads were used to minimize the electrolyte volume. Before use, the carbon films with a weight loading of  $15 \text{ mg cm}^{-2}$  were placed onto Pt disk used as current collectors. The cell was assembled in a glove box operated under Ar atmosphere (water and oxygen content below 0.1 ppm), and filled with acetonitrile + 1.5 M  $\text{Et}_4\text{NBF}_4$  electrolyte. The cell was then sealed with epoxy resin (EA 3463, LOCTITE) and placed in a FIBOX (FIBOX FEX PC-7 Enclosure) to ensure airtightness, and then removed from the glove box to be tested.

## 2.2. Surface functional groups titration by the Boehm's method

Raw porous carbon powders (binder-free) were analyzed by the Boehm's method. Three suspensions of activated carbon were prepared by adding  $30 \text{ g L}^{-1}$  of activated carbon powder in three alkaline solutions at 0.1 M of  $\text{HCO}_3\text{Na}$  (pKa 6.4),  $\text{NaCO}_3$  (pKa 10.3) and NaOH (pKa 15.7). After 12 h of stirring, the solution was filtered. 20 mL of the filtered solution was titrated by 0.1 M hydrochloric acid. From the titration curves, acidic functions can be classified into three groups of decreasing acidity strength according to Boehm et al. [13] (Fig. 1). According to Yoshida et al. [14], basic surface functions has less impact on the performance of supercapacitors than acidic ones. For this reason, the total basic functions are all titrated by preparing a 0.1 M hydrochloric acid carbon suspension. The amount of hydrochloric acid remaining after 12 h was dosed with 0.1 M NaOH. Basic surface functions of commercial activated are linked with the presence of electron- $\pi$  delocalization in the graphene network, for example: chromenes, ketones and pyrone [15].

## 2.3. Temperature-programmed desorption coupled with mass spectrometry (TPD-MS)

The carbon electrode samples were placed in a quartz tube in an oven under vacuum. The heating rate was  $5^\circ\text{C min}^{-1}$ , in a temperature range between  $25^\circ\text{C}$  and  $900^\circ\text{C}$ . When the temperature reaches  $900^\circ\text{C}$ , the sample is maintained at this temperature for 30 min. During the thermal treatment, the released gases from the materials are continuously analyzed by mass spectroscopy to determine the gas composition.

## 3. Results and discussion

### 3.1. Titration by the Boehm's method

Boehm's method was used to titrate the functional groups present on the surface of as-received carbons. From the titration curves, acid functions can be classified into three groups of decreasing acidity strength [13] (Fig. 1).

Table 2 summarizes the titration results. As-received carbon A has mainly basic functions with some phenolic acid function, while carbon B exhibits a much higher phenolic acid function content (almost 3 times more), whereas it has got a similar quantity of basic functions. Overall, the Carbon B has clearly a higher amount of acidic functional groups than the carbon A.

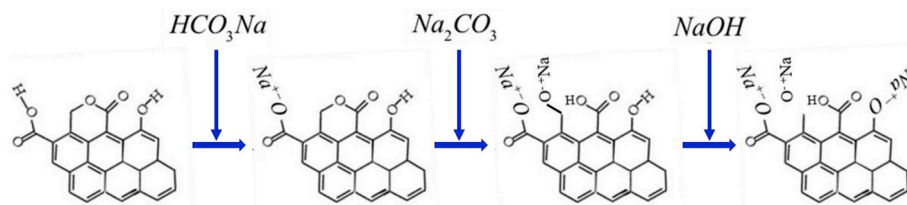


Fig. 1. Example of titration according to Boehm's classification [13].

Table 2

Results of titration Boehm where the quantity and the type of surface functional group is detailed.

Carbon name	Quantity of surface functional groups
A (YP-50F)	Phenol $0.09 \text{ mmol g}^{-1}$
	Basic functions $0.27 \text{ mmol g}^{-1}$
B	Phenol $0.33 \text{ mmol g}^{-1}$
	Basic functions $0.23 \text{ mmol g}^{-1}$

### 3.2. TPD-MS analysis results

Temperature-programmed desorption coupled with mass spectrometry technique (TPD-MS) was used in complement to the Boehm's method to determine more finely the surface functional groups present on the carbon surface. TPD-MS is more sensitive than Boehm method (analysis under vacuum and detected by mass spectrometry). In our experiments, we mainly focused onto the evolution of CO and  $\text{CO}_2$  gases during the heat treatment from room temperature to  $900^\circ\text{C}$ . The temperature at which the gases are released gives information about the nature of the surface functional groups present onto the carbon surface (see Fig. 2).

The presence of 5 wt% PTFE in the electrodes leads to a consequent release of gaseous species ( $\sim 550^\circ\text{C}$ ) during the TPD-MS analysis (see Fig. S1, Supplementary Information), which comes with two important drawbacks. First, the set of results obtained from TPD-MS analysis is not quantitative here but semi-quantitative only, that explains why the intensity of detected gases is given in  $\text{A.g}^{-1}$ . Second, the detected  $\text{M/z} = 28$  and  $\text{M/z} = 44$  mainly assigned to CO and  $\text{CO}_2$ , respectively, can also come from PTFE decomposition. To remove the contribution of PTFE, the intensity of the gas detection signal was normalized according to the following equation:

$$I_{\text{norm}} = \frac{I_{\text{exp}}}{I_{\text{PTFE}}} \quad (4)$$

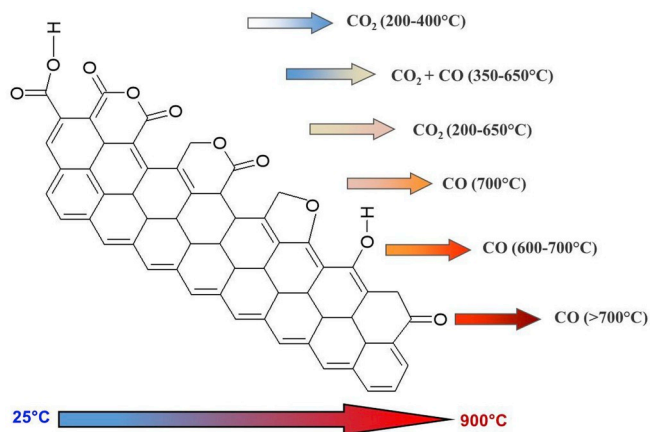


Fig. 2. Correspondence between the oxygen-based surface functions and the nature of desorbed gases at different temperature during TPD-MS analysis. Schema redraw based on the work of Figueroa [16].

where  $I$  correspond to the measured intensity (Ampere per gram) and  $I_{\text{exp}}$  is the experimental signal. The contribution of PTFE can be found as follows:  $I_{\text{PTFE}} = I_{\text{carbon+PTFE}} - I_{\text{carbon}}$ . Here,  $I_{\text{carbon+PTFE}}$  is the signal of the raw carbon with PTFE and  $I_{\text{carbon}}$  is the intensity of the raw carbon. Our normalized TPD-MS signal  $I_{\text{norm}}$  is obtained by subtracting the contribution of PTFE ( $I_{\text{PTFE}}$ ) to the experimental signal  $I_{\text{exp}}$ .

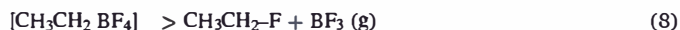
### 3.2.1. TPD-MS analysis of carbon A

Fig. 3 shows the normalized TPD-MS analysis results for masses  $M/z$  28,  $M/z$  44,  $M/z$  27 and  $M/z$  20 for carbon A.

The CO ( $M/z$  28) released from initial (raw) carbon A increases from 700°C without obvious presence of  $\text{CO}_2$  ( $M/z$  44). According to Fig. 2, phenol, ether and carbonyl surface functions are present on the initial carbon A before ageing. This information confirms results of Boehm titration (Table 2), however, carbonyl functions, which are less acidic than phenol groups, could not be distinguished through Boehm's method.

Moving to aged electrodes, both positive and negative aged carbon electrodes release a significantly larger amount of species with  $M/z$  28 and  $M/z$  44 than the initial (raw) carbon. However, the attribution of  $M/z$  28 and  $M/z$  44 peaks is more complex, since other species than CO and  $\text{CO}_2$ , respectively, are contributing to this mass especially in the lower temperature range ( $T < 400^\circ\text{C}$ ). More precisely, the electrolyte salt  $\text{Et}_4\text{NBF}_4$  can decompose into TriEthyl Amine (TEA)  $\text{N}(\text{C}_2\text{H}_5)_3$  as an intermediate product, which, by elimination reactions forms ethylene,  $\text{CH}_2=\text{CH}_2$  ( $M/z$  28) and  $\text{BF}_3$  ( $M/z$  49) species according to Eqs. (5) and (6) [17]. The TriEthyl Amine (TEA) decomposition is accompanied by simultaneous release of other masses, i.e.,  $M/z$  27 ( $\text{CH}_2-\text{CH}$ ),  $M/z$  29 ( $\text{CH}_3-\text{CH}_2$ ),  $M/z$  30 ( $\text{CH}_2=\text{NH}_2$ ),  $M/z$  42 ( $\text{C}_2\text{H}_4-\text{N}^+$ ),  $M/z$  44 ( $\text{CH}_3\text{CH}_2\text{N}^+\text{H}$ ),  $M/z$  58 ( $\text{CH}_2=\text{NH}^+\text{C}_2\text{H}_5$ ),  $M/z$  86 ( $(\text{C}_2\text{H}_5)_2\text{N}^+\text{CH}_2$ ) and  $M/z$  101 ( $\text{N}^+(\text{C}_2\text{H}_5)_3$ ) [18,19], as observed in the mass spectra of aged carbon A (Figure S2 and S3, SI) at  $T < 400^\circ\text{C}$ . This confirm the decomposition of electrolyte TEA species, in good agreement with other works [17]. Another pathway of electrolyte decomposition can be achieved by nucleophilic substitution reactions

which may lead to  $\text{C}_2\text{H}_5-\text{F}$  ( $M/z$  47) and  $\text{BF}_3$  ( $M/z$  49) species [20] (Eqs. (7) and (8)).



Compared to raw electrode (before ageing), larger amounts of both  $M/z$  28 and 44 were found to be released at the positive electrode after ageing. Beyond  $400^\circ\text{C}$ , the masses  $M/z$  28 and 44 are mainly due to CO and  $\text{CO}_2$  coming from oxygen functional groups, suggesting a more advanced oxidation of the positive electrode during ageing. This is in agreement with our previous work based on TG-IR and Raman spectroscopy analyses, showing that positive electrodes suffer from more important oxidation than negative electrode after ageing [8]. According to Figs. 2 and 3, most of oxygenated surface functions are present at both positive and negative electrode surface after ageing: basic groups (lactone, ether, phenol and carbonyl) are released as CO at higher temperatures ( $>400^\circ\text{C}$ ) while acidic groups (carboxylic, anhydride) which are released as  $\text{CO}_2$  or concomitantly with CO species at low temperatures ( $<400^\circ\text{C}$ ). The latter groups are more difficult to discriminate since the signal of  $\text{CO}_2$  is overlapped with that of the TEA from the electrolyte salt (same  $M/z$  44) [17].

The mass  $M/z$  27 and  $M/z$  20 were also detected for the raw and aged electrodes during the TPD-MS analysis; it corresponds mainly to HCN and traces of HF which are assumed to come from the decomposition of the electrolyte (acetonitrile and  $\text{BF}_3$ , respectively) during heating. Once again, the intensity of these species is more important for the positive electrode than the negative one. The important HCN release from the positive electrode between  $400^\circ\text{C}$  and  $880^\circ\text{C}$  is assumed to come from the decomposition of polymerized acetonitrile species, linked to some extent to the higher oxidation of the positive carbon which favor the adsorption of the electrolyte solvent via the new formed oxygen

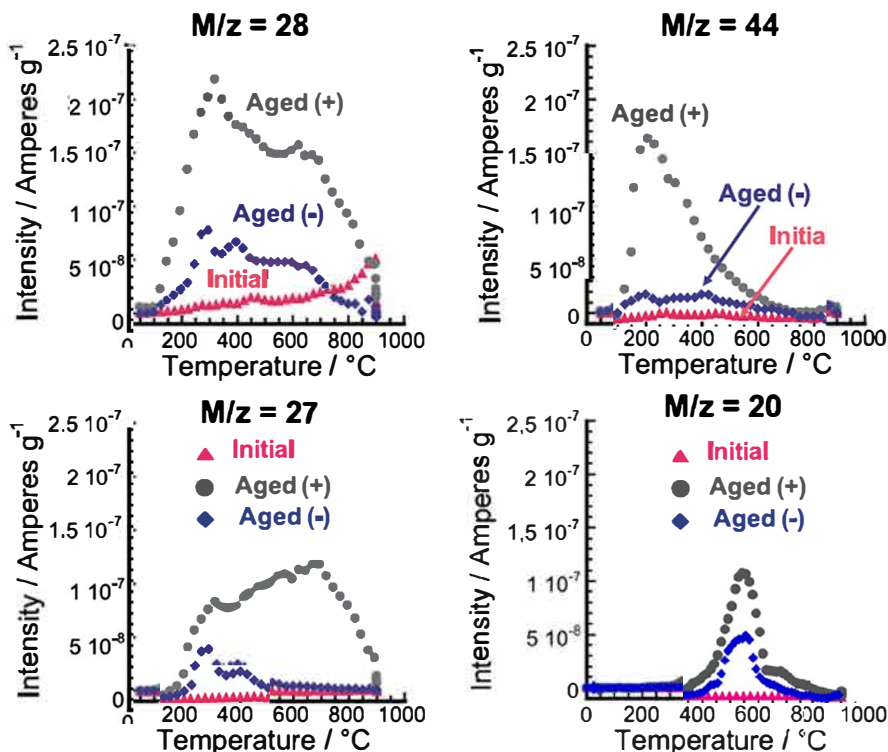


Fig. 3. TPD-MS results for raw (initial) and aged carbon A electrodes, for masses  $M/z$  = 28,  $M/z$  = 44,  $M/z$  = 27 and  $M/z$  = 20.

functional groups. Taking into account that the ageing is done in non-aqueous electrolyte, it can be proposed that the defects on the carbon surface are firstly created during cycling due to the interactions of carbon with  $\text{BF}_4^-$  species, which serve as anchoring sites for electrolyte molecules and once the material exposed to air, to oxygen functional groups creation.

From these results, we can conclude that after ageing, carbon electrodes became more hydrophilic because of the presence of oxygen functional groups. The presence of trace of HF confirm the hydrolysis or partial hydrolysis of  $\text{BF}_4^-$  during ageing [9].

### 3.2.2. TPD-MS analysis of carbon B

Differently from carbon A, the raw carbon B contains anhydride functional groups as can be seen from the  $\text{CO}_2$  ( $M/z$  44) and CO ( $M/z$  28) peaks in the  $400^\circ\text{C}$ – $600^\circ\text{C}$  temperature range in Fig. 4. No increase in CO group (raw carbon B) at high temperature is noticed, suggesting less basic carbon surface functional groups. Results from the titration by the Boehm method in Table 2 showed an important content of phenol functions on carbon B. Although the slight difference in acidity between anhydride functions and phenol functions makes it difficult to distinguish between those two groups by Boehm's titration method. These results confirm that the surface groups present onto raw carbon B before ageing are more acidic than carbon A.

Then, unlike carbon A, there is no major difference of intensity between the positive electrode and the negative electrode after ageing for carbon B (Fig. 4); however, aged carbons were found to release more gaseous species compared to the (raw) initial carbon. The most intense peaks are observed for  $M/z$  28.

For the negative electrode, two well defined peaks are observed at  $\sim 280^\circ\text{C}$  and  $\sim 400^\circ\text{C}$ . A closer look in this temperature range (see Figs. S4 and S1) suggests an origin from the decomposition fragments of electrolyte (TEA) according to Eqs. (5)–(8) and of polyacetonitrile (P-ACN on Fig. S4 S1), respectively. The polyacetonitrile could be formed on the carbon surface by polymerization of acetonitrile solvent (Eq. (3)). Its decomposition in this temperature range is consistent with some TGA

results reported in the literature, showing high stability of such compound below  $300^\circ\text{C}$  and a decomposition beyond  $400^\circ\text{C}$  [21]. The main decomposition species of this polymer are the ethylene ( $M/z$  28), hydrogen cyanide HCN ( $M/z$  27),  $\text{C}_2\text{H}_5$  ( $M/z$  29) and  $\text{CH}_2\text{CHCN}$  ( $M/z$  42) as seen in Figs. S4 and S1 and other works [22].

Considering the positive electrode (Figs. S4 and S1), the aforementioned peak observed at  $280^\circ\text{C}$  (TEA) is no longer visible but the peak at  $400^\circ\text{C}$  is still present; a second peak shows up at higher temperature range ( $\sim 700^\circ\text{C}$ ). The disappearance of the  $280^\circ\text{C}$  peak may be related to the fact that TEA species are mainly adsorbed on the negative electrode during cycling while  $\text{BF}_4^-$  species are mainly located on the positive electrode. The last peak at high temperature can be related mainly to CO groups.

For both negative and positive electrodes, the  $M/z$  28 signal for  $T > 600^\circ\text{C}$  is much higher than that of pristine carbon. Taking into consideration that at this temperature range most of the electrolyte/solvent species have already decomposed, it is likely that the observed  $M/z$  are linked to CO coming from basic oxygen functional groups release, therefore, a higher degree of oxidation after cycling. According to Fig. 2, in this temperature range mainly ether, phenol and quinone groups are identified [23]. Interestingly, the positive electrode was found to be more oxidized than the negative one as demonstrated by the intense and well defined peak at around  $700^\circ\text{C}$ , indicating high amounts of ether and phenol groups.

For the  $M/z$  44, a broad peak is observed between  $200$  and  $500^\circ\text{C}$  for both positive and negative electrode (Fig. 4). As mentioned for Carbon A, it is difficult to distinguish between the decomposition of electrolyte salt or/and  $\text{CO}_2$  coming from surface functional groups. In addition, the  $M/z$  27 mass signal of the negative electrode is split into two peaks at  $\sim 250^\circ\text{C}$  and  $\sim 500^\circ\text{C}$  which can be associated to decomposition fragments of TriEthyl Amine (TEA) and HCN release, respectively. For the positive electrode, the sole HCN contribution is seen, suggesting once again that TEA is mainly found in the negative electrode. Contrastly to carbon A, a HCN release is observed for carbon B on both positive and negative electrodes. The release of species  $M/z$  20

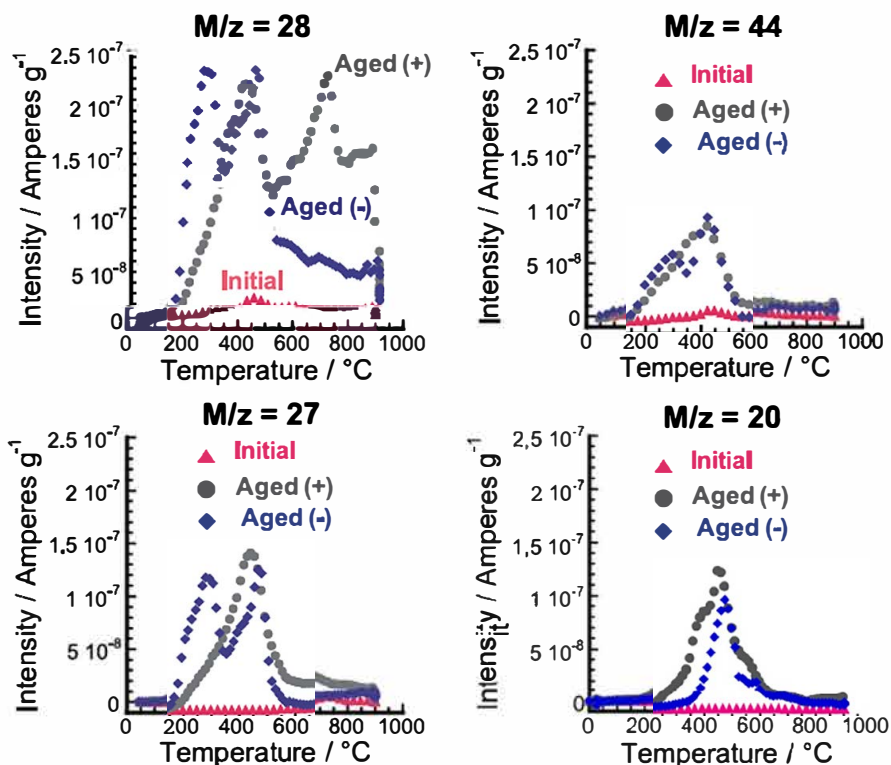


Fig. 4. TPD-MS results for raw (initial) and aged carbon B electrodes, for masses  $M/z$  = 28,  $M/z$  = 44,  $M/z$  = 27 and  $M/z$  = 20.

signal is associated to HF coming from  $\text{BF}_4$  (Eq. (6)) which occurs around  $400^\circ\text{C}$  (the PTFE decomposition takes place at slightly higher temperature, see Figs. S1 and SI). As observed, the HF peak is larger at the positive electrode, suggesting a stronger interaction of  $\text{BF}_4^-$  ions with the positive electrode. As a result, this may explain the higher oxidation observed on the positive electrode [24].

In summary, TPD-MS analysis shows that carbons A and B are all oxidized after electrochemical ageing tests. Particularly, carbon B looks to be further oxidized upon cycling according to the presence of mainly basic functional groups; the acidic groups being more difficult to discriminate due to the electrolyte decomposition at the same temperature range. Moreover, the negative electrode was found to be less oxidized than the positive one and to release decomposed TEA molecule whereas at the positive electrode the presence of  $\text{BF}_3$  HF was unveiled. Interestingly, on both positive and negative electrodes, the existence of a polyacetonitrile polymer layer was evidenced on carbon B on both positive and negative electrode and not observed on carbon A.

### 3.3. Electrochemical tests at constant potential using two-compartment cell

A two-compartment cell design has been used, previously proposed by Ishimoto et al. [25] to study the influence of the water content on the ageing behavior of the positive and negative electrode, separately. This study has been focused on carbon A since, as found previously, it has turned out that it becomes more hydrophilic after ageing. These cells have been assembled with carbon A, with different water content in a 1.5 M  $\text{NET}_4\text{BF}_4$  in ACN electrolyte. The cell potential was set at 2.5 V. PVDF binder was used in these experiments to cast carbon films directly onto the Pt current collector, to ensure a better active material adherence. Electrolyte of Cell#1 has 250 ppm water content in both positive (anolyte) and negative (catholyte) compartment while electrolyte of Cell#2 has 2500 ppm water content. Each cell compartment was initially filled out with 18 mL of electrolyte. The images in Fig. 5 show that the anolyte of Cell#2 ( $[\text{H}_2\text{O}]_{t=0}; 2500 \text{ ppm}$ ) becomes yellow-colored after only three days of floating test.

The change of the leakage currents of each cell versus ageing time (center panel) was monitored as seen in Fig. 5. As expected, the leakage current increases with the water content in the electrolyte evidencing that the electrolyte water content plays a significant role in the ageing mechanisms of carbon electrode. As mentioned before, Bittner et al. [7] found a correlation between the coloration of the electrolyte and the formation of a polyacetonitrile polymer  $-\text{[N}=\text{C}(\text{CH}_3)]_n-$  onto the carbon electrode from XPS analysis [5–7]. The polymer was found to be formed preferentially at the positive electrode. It could then be assumed that the yellow species formed at the positive electrode are soluble short polymer chains or oligomers of polyacetonitrile polymer  $-\text{[N}=\text{C}(\text{CH}_3)]_n-$ .

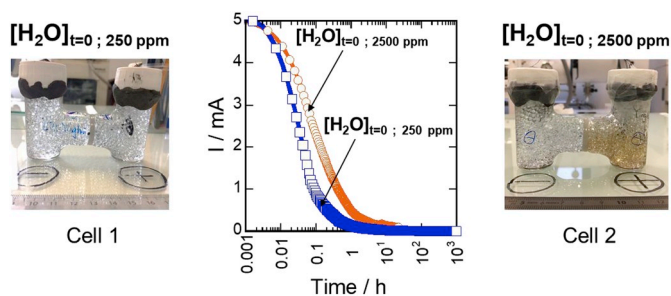


Fig. 5. Change of the leakage currents with time during floating at 2.5 V of two cells assembled with separate compartments (center), containing 250 ppm (left) and 2500 ppm (right) of water in the electrolyte.

## 4. Carbon-based supercapacitor's ageing mechanisms hypothesis

The set of results obtained here is consistent with our previous work [8] and allows for proposing a possible ageing mechanism. Our previous work based on the combination of Electrochemical Impedance Spectroscopy (EIS) analysis, Raman and Infrared spectroscopies showed two different ageing mechanisms for carbon A and carbon B. An increase of the interface resistance of supercapacitor B allowed to propose the formation of a protective, passive-like layer at the surface of carbon B.

Results obtained using the surface group analysis by Boehm and bulk TPD-MS technique can help in going further into the details of the ageing mechanisms. For the positive electrode of both carbon A and B, the increase of surface functional group content is more important than that of the negative electrode. For carbon B, the oxygen surface group content is more important on the aged electrode compared to rawcarbon. It suggests that the protective layer formed on carbon B mainly depends on the nature and content of the functional groups present at the carbon surface. Besides, results obtained using two-compartment cells with carbon A suggest a polymerization process onto the carbon surface at the positive electrode during floating test. This analysis also confirms that the presence of water accelerates the carbon ageing process.

Based on the present TPD-MS study and previous results [8], we propose two different ageing mechanisms for carbons A and B. Both mechanisms share a common first step which consists in the formation of a super-acid  $\text{HF-BF}_3$  at the positive electrode, coming from the hydrolysis of  $\text{BF}_4^-$  in presence of traces of water in the electrolyte, as already proposed by Kurzweil et al. as described by following equations [9]. By diffusion, a part of  $\text{HF-BF}_3$  can go to the negative electrode.



In carbon A (Fig. 6 a), the formation of the super-acid is more important at the positive electrode. The superacid and/or HF oxidize the carbon resulting in defects creation, which further react with water traces present in the electrolyte to form surface functions such as carboxylic, anhydride, lactone, ether, phenol and carbonyl groups. The appearance of yellow color in the anolyte suggests that soluble polyacetonitrile oligomers are created by reaction between  $\text{BF}_4^-$  radical formed at high potentials and acetonitrile at the positive electrode [7, 10].

For carbon B (Fig. 6 b), the ageing mechanism also starts with the hydrolysis of  $\text{BF}_4^-$  in presence of traces of water. However, a protective, ionically-conductive and electronically resistive passive-like layer is formed on the surface of carbon as observed by TPD-MS which protects the carbon surface from further oxidation and avoids structural change [8]. Results of TPD-MS suggest that the formation of the protective layer on positive and negative electrode is possible thanks to the presence of acidic groups like carboxylic groups or anhydride functional groups which could subsequently hydrolyzed into carboxyl functions in the presence of water (Fig. 6 b) onto the surface of pristine carbon. It is then assumed that soluble created polyacetonitrile oligomers can form an insoluble polymer onto the carbon surface of carbon B via the creation of hydrogen bonds, leading to the presence of a passive-like polymer film onto the surface of carbon grains (Fig. 6 b).

## 5. Conclusion

In this article, we used TPD-MS and electrochemical tests at constant potential using two-compartment cell to unveil details of two different mechanisms studied in our previous work.

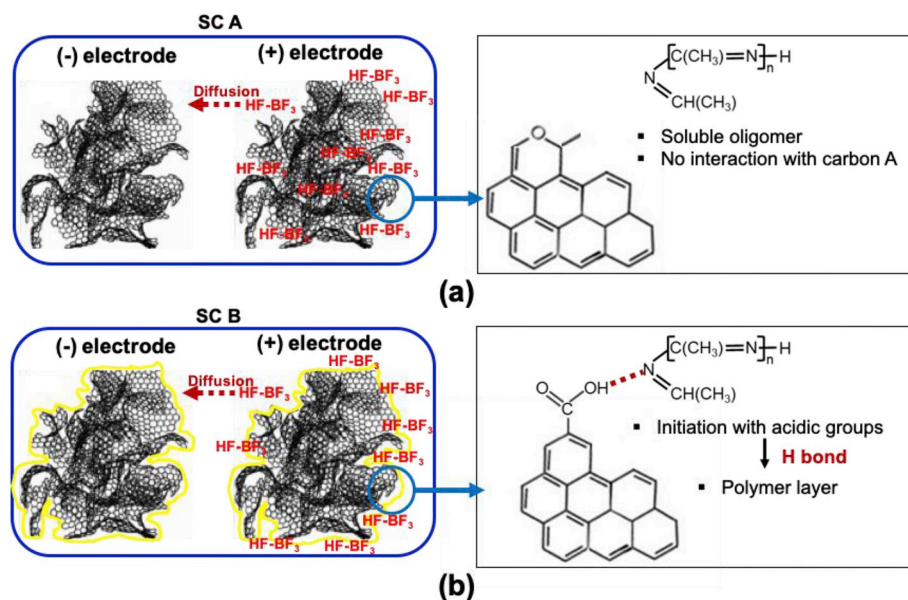


Fig. 6. Proposed ageing mechanisms for SC A and SC B during electrochemical ageing in supercapacitor cells, using a carbon structure proposed by Terzyk et al. [26].

Results of TPD-MS analysis showed that both electrodes based on carbon A and carbon B were oxidized after electrochemical ageing. For both carbon A and B, the positive electrode was found to be more oxidized than the negative one; both aged electrodes were more oxidized than the initial carbon ones. Fragments of TEA and HCN release were observed on the negative electrode on both carbons while a polyacetonitrile polymer was evidenced mainly on carbon B. Additionally, HF is detected on both aged electrodes A and B where the content of HF is more important on positive electrodes.

Electrochemical tests at constant potential using two-compartment cell revealed two ageing factors. First, the electrolyte water content plays a significant role in the ageing mechanisms of supercapacitors. Second, a yellow-colored electrolyte product is observed only in anolyte and related to poly-acetonitrile polymer  $-\text{[N=C(CH}_3\text{)]}_n-$  compounds.

Based on the present TPD-MS study, two different ageing mechanisms for carbons A and B have been proposed.

For SC A, the hydrolysis of  $\text{BF}_4^-$  occurred in the positive electrode during the ageing and it produces the  $\text{HF-BF}_3$  (super acid) and HF. This super acid/HF caused the formation of defects in the carbon network (where Raman results showed the positive electrode is significantly more disordered than the negative electrode) which are reactive towards the formation of oxygen functional groups. Corroborated with the high voltage, the presence of  $\text{BF}_4^-$  can initiate the polymerization of acetonitrile at the positive electrode. This polymerization produces a soluble oligomer which caused the yellow coloration. The hydrolysis of  $\text{BF}_4^-$  and the polymerization also happened at the positive electrode of SC B (yellow coloration of washed electrodes). The acid surface functional groups probably attracted the oligomer derived from acetonitrile polymerization and form a protective layer on the surface of carbon B.

#### CRedit authorship contribution statement

**Yinghui Liu:** Conceptualization, Resources, Investigation, Methodology, Writing - original draft. **Bénédicte Réty:** Formal analysis, Investigation, Methodology. **Camélia Matei Ghimbeu:** Formal analysis, Validation, Writing - review & editing. **Benoît Soucaze-Guillous:** Funding acquisition. **Pierre-Louis Taberna:** Conceptualization, Investigation, Methodology, Validation, Supervision, Writing - review & editing. **Patrice Simon:** Project administration, Visualization, Formal analysis, Conceptualization, Methodology, Validation, Resources, Supervision, Writing - review & editing.

#### Acknowledgements

We thank the team “Carbon and Hybrid Materials” in Science of Material Institute in Mulhouse (IS2M) for the help with TPD-MS analyses, particularly, Joseph Dentzer is acknowledged for useful discussions. P. Simon and P.-L. Taberna thanks the Renault Company for funding as well as the ANR (LABEX STORE-EX). Y. Liu PhD thesis was supported by a grant from the Renault Company (CIFRE N° 2014/0557).

#### Appendix A. Supplementary data

Supplementary data to this article can be found online at <https://doi.org/10.1016/j.jpowsour.2019.226734>.

#### References

- [1] J.R. Miller, P. Simon, Electrochemical capacitors for energy management, *Science* 321 (5889) (Aug. 2008) 651–652.
- [2] Maxwell Technologies Ultracapacitors, Supercapacitors, Microelectronics and High Voltage,” Maxwell Technologies. [Online]. Available: <http://www.maxwell.com/default.aspx>. [Accessed: 16-Jan-2019].
- [3] Y. Gogotsi, P. Simon, True performance metrics in electrochemical energy storage, *Science* 334 (6058) (Nov. 2011) 917–918.
- [4] J.R. Miller, Engineering electrochemical capacitor applications, *J. Power Sources* 326 (Sep. 2016) 726–735.
- [5] P. Azais, et al., Causes of supercapacitors ageing in organic electrolyte, *J. Power Sources* 171 (2) (Sep. 2007) 1046–1053.
- [6] M. Zhu, et al., Chemical and electrochemical ageing of carbon materials used in supercapacitor electrodes, *Carbon* 46 (14) (Nov. 2008) 1829–1840.
- [7] A.M. Bittner, et al., Ageing of electrochemical double layer capacitors, *J. Power Sources* 203 (Apr. 2012) 262–273.
- [8] Y. Liu, B. Soucaze-Guillous, P.-L. Taberna, P. Simon, Understanding of carbon-based supercapacitors ageing mechanisms by electrochemical and analytical methods, *J. Power Sources* 366 (Oct. 2017) 123–130.
- [9] P. Kurzweil, M. Chwistek, Electrochemical stability of organic electrolytes in supercapacitors: spectroscopy and gas analysis of decomposition products, *J. Power Sources* 176 (2) (Feb. 2008) 555–567.
- [10] G. Tourillon, P.-C. Lacaze, J.-E. Dubois, Electrochemical formation of thin polyacetonitrile films on a Pt surface: P.m.t., i.r., x.p.s. and s.i.m.s. analyses and study of formation mechanism, *J. Electroanal. Chem. Interfacial Electrochem.* 100 (1) (Jun. 1979) 247–262.
- [11] N. Jackel, P. Simon, Y. Gogotsi, V. Presser, Increase in capacitance by subnanometer pores in carbon, *ACS Energy Lett.* 1 (6) (Dec. 2016) 1262–1265.
- [12] S. Ishimoto, Y. Asakawa, M. Shinya, K. Naoi, Degradation responses of activated-carbon-based EDLCs for higher voltage operation and their factors, *J. Electrochem. Soc.* 156 (7) (Jul. 2009) A563–A571.
- [13] H.P. Boehm, Chemical identification of surface groups, in: D.D. Eley, H. Pines, P. B. Weisz (Eds.), *Advances in Catalysis*, vol. 16, Academic Press, 1966, pp. 179–274.

- [14] A. Yoshida, I. Tanahashi, A. Nishino, Effect of concentration of surface acidic functional groups on electric double-layer properties of activated carbon fibers, *Carbon* 28 (5) (Jan. 1990) 611–615.
- [15] M.A. Montes-Morán, D. Suárez, J.A. Menéndez, E. Fuente, On the nature of basic sites on carbon surfaces: an overview, *Carbon* 42 (7) (Jan. 2004) 1219–1225.
- [16] J.L. Figueiredo, M.F.R. Pereira, M.M.A. Freitas, J.J.M. Órfao, Modification of the surface chemistry of activated carbons, *Carbon* 37 (9) (Jan. 1999) 1379–1389.
- [17] "Chapter-7: Thermal Decomposition of Pure Compounds of Tetraalkylammonium Tetrafluoroborates (R<sub>4</sub>NBF<sub>4</sub>)." [Online]. Available: [http://shodhganga.inflibnet.ac.in/bitstream/10603/64438/15/15\\_chapter%207.pdf](http://shodhganga.inflibnet.ac.in/bitstream/10603/64438/15/15_chapter%207.pdf).
- [18] M.R.R. Prasad, K. Sudhakarbabu, B. Sreedhar, D.K. Devi, A simultaneous TG-DTG-DSC-quadrupole mass spectrometric study, *J. Therm. Anal. Calorim.* 116 (2) (May 2014) 1027–1031.
- [19] J. Mohan, *Organic Spectroscopy: Principles and Applications*, 2000.
- [20] M.R.R. Prasad, K. Sudhakarbabu, Thermal decomposition of tetraethyl ammonium tetrafluoroborate, *J. Therm. Anal. Calorim.* 115 (2) (Feb. 2014) 1901–1905.
- [21] F. Li, et al., Synthesis and characterization of a cyclic polyacetonitril oligomer and its application on solid polymer electrolyte, *Int J Electrochem Sci* 10 (15) (2015).
- [22] P.F. Britt, *Pyrolysis and Combustion of Acetonitrile (CH<sub>3</sub>CN)*, Prepared by OAK RIDGE NATIONAL LABORATORY Oak Ridge, Tennessee 37831-6285 Managed by UT-BATTELLE, LLC for the U.S. DEPARTMENT OF ENERGY under contract DE-AC05-00OR22725, 2002.
- [23] G. Moussa, C. Matei Ghimbeu, P.-L. Taberna, P. Simon, C. Vix-Guterl, Relationship between the carbon nano-onions (CNOs) surface chemistry/defects and their capacitance in aqueous and organic electrolytes, *Carbon* 105 (Aug. 2016) 628–637.
- [24] M. Vijayaraj, et al., The influence of surface chemistry and pore size on the adsorption of proteins on nanostructured carbon materials, *Adv. Funct. Mater.* 20 (15) (2010) 2489–2499.
- [25] S. Ishimoto, Y. Asakawa, M. Shinya, K. Naoi, Degradation responses of activated-carbon-based EDLCs for higher voltage operation and their factors, *J. Electrochem. Soc.* 156 (7) (Jul. 2009) A563–A571.
- [26] A.P. Terzyk, et al., How realistic is the pore size distribution calculated from adsorption isotherms if activated carbon is composed of fullerene-like fragments? *Phys. Chem. Chem. Phys.* 9 (44) (2007) 5919–5927.

## Supplementary Informations

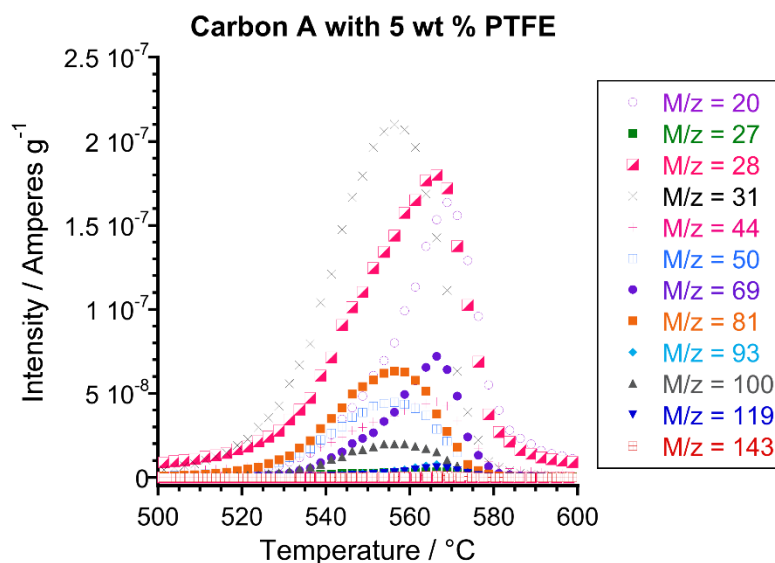


**Figure S1:** TPD-MS desorption curves for Carbon A (YP-50F) before ageing showing the main masses  $m/z$  resulting from PTFE decomposition

According to Figure S1, the presence of 5 wt% PTFE in carbon electrodes release a consequent quantity of gaseous species around 550 °C during TPD-MS analysis.

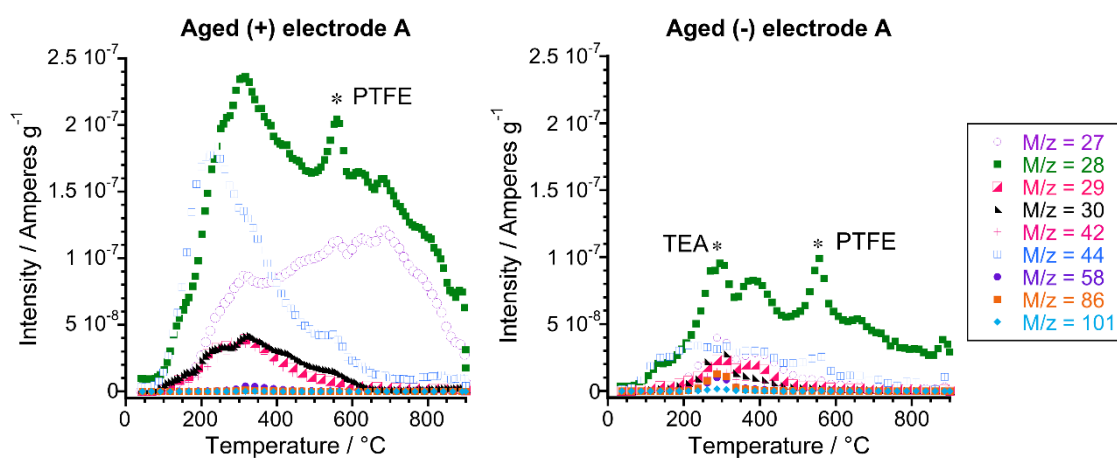


**Figure S2:** TPD-MS profiles of Carbon A (YP-50) positive and negative electrodes before normalization according to equation (4) used to remove the contribution of PTFE

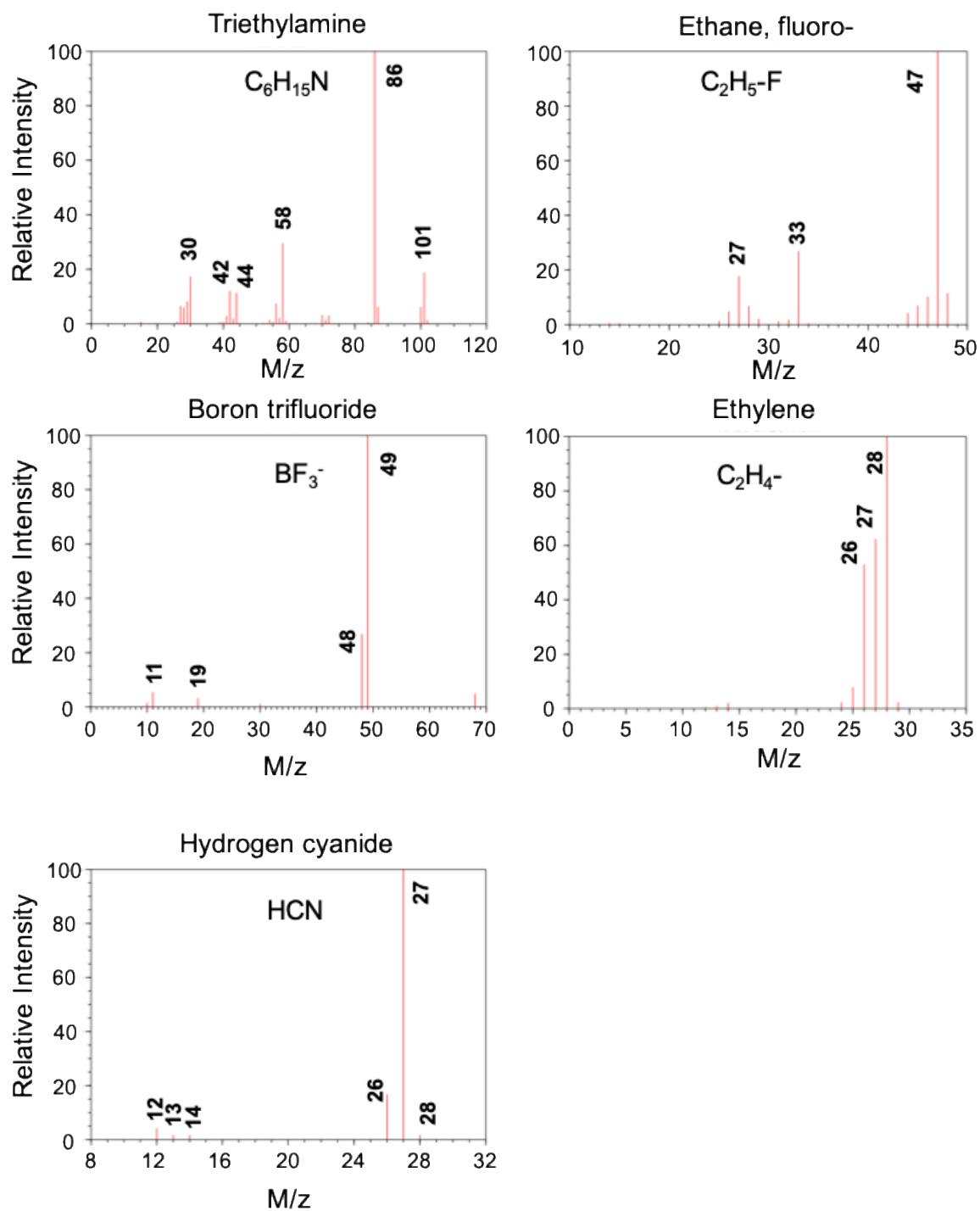


**Figure S3:** Mass spectra of (a) triethylamine, (b) ethane, fluoro-, (c) boron trifluoride, (d) ethylene and (e) hydrogen cyanide (source: NIST Chemistry WebBook, <https://webbook.nist.gov/chemistry>)

According to Figure S2 and S3, components of decomposed electrolyte species are observed in the mass spectra of aged Carbon A. Peaks at 300 °C of  $M/z = 28, 44, 86,$  and  $101$  proved the presence of TriEthyl Amine (TEA) on aged negative electrode A.

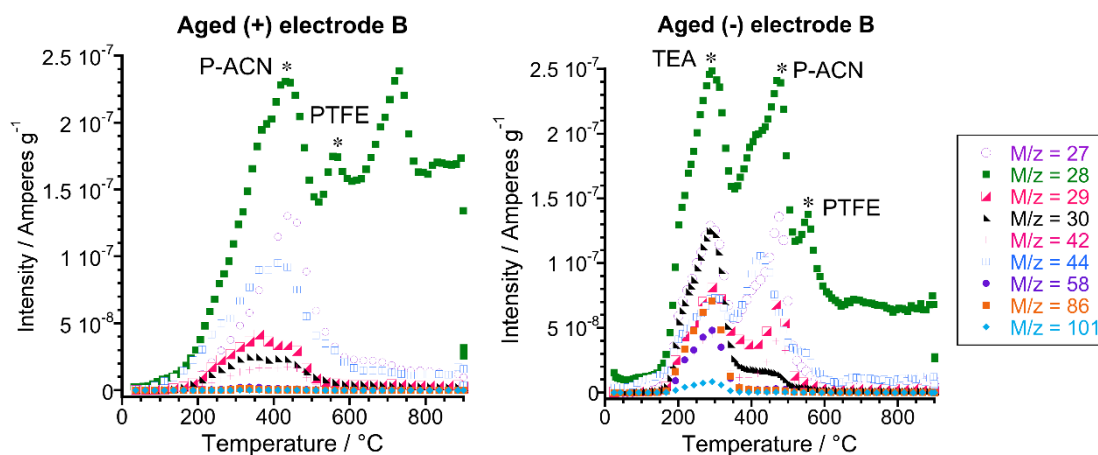


**Figure S4:** TPD-MS profiles of Carbon B positive and negative electrodes showing the main masses released during heating.

According to Figure S4, the polyacetonitrile (P-ACN) is present on both positive and negative aged electrode B by polymerization of acetonitrile solvent. Peaks observed at 280 °C of  $M/z = 28, 30, 42, 58$  and  $101$  evidenced the presence of Triethyl Amine (TEA) on aged negative electrode B. While the peaks at 280 °C are absent on aged positive electrode B, it can be related to the fact that TEA species are mainly adsorbed on the negative electrode during cycling while  $\text{BF}_4^-$  species are mainly located on the positive electrode.